N2CLS: the NIKA2 view of the distant Universe

S. Berta[1], R. Adam[2], P. Ade[3], H. Ajeddig[4], S. Amarantidis[5], P. André[4], H. Aussel[4], A. Beelen[6], A. Benoît[7], M. Béthermin[8], A. Bongiovanni[5], J. Bounmy[9], O. Bourrion[9], M. Calvo[7], A. Catalano[9], D. Chérouvrier[9], M. De Petris[10], F.-X. Désert[11], S. Doyle[3], E. F. C. Driessen[1], G. Ejlali[12], A. Ferragamo[10], A. Gomez[13], J. Goupy[7], C. Hanser[14], S. Katsioli[15,16], F. Kéruzoré[17], C. Kramer[1], B. Ladjelate[5], G. Lagache[6], S. Leclercq[1], J.-F. Lestrade[18], J. F. Macías-Pérez[9], S. C. Madden[4], A. Maury[19,20,4], F. Mayet[9], A. Monfardini[7], A. Moyer-Anin[9], M. Muñoz-Echeverría[21], I. Myserlis[5], A. Paliwal[22], L. Perotto[9], G. Pisano[10], N. Ponthieu[11], V. Revéret[4], A. J. Rigby[23], A. Ritacco[9], H. Roussel[24], F. Ruppin[25], M. Sánchez-Portal[5], S. Savorgnano[9], K. Schuster[1], A. Sievers[5], C. Tucker[3], and R. Zylka[1]

[1]Institut de RadioAstronomie Millimétrique (IRAM), Saint Martin d'Hères, France
[2]Univ. Côte d'Azur, Observatoire de la Côte d'Azur, CNRS, Laboratoire Lagrange, France
[3]School of Physics and Astronomy, Cardiff University, Queen's Buildings, The Parade, Cardiff, CF24 3AA, UK
[4]Univ. Paris Cité, Université Paris-Saclay, CEA, CNRS, AIM, F-91191 Gif-sur-Yvette, France
[5]Institut de Radioastronomie Millimétrique (IRAM), Avenida Divina Pastora 7, Granada, Spain
[6]Aix Marseille Univ, CNRS, CNES, LAM (Laboratoire d'Astrophysique de Marseille), Marseille, France
[7]Institut Néel, CNRS, Université Grenoble Alpes, France
[8]Univ. de Strasbourg, CNRS, Observatoire astronomique de Strasbourg, 67000 Strasbourg, France
[9]Univ. Grenoble Alpes, CNRS, LPSC-IN2P3, 53, av. des Martyrs, 38000 Grenoble, France
[10]Dipartimento di Fisica, Sapienza Università di Roma, Piazzale Aldo Moro 5, I-00185 Roma, Italy
[11]Univ. Grenoble Alpes, CNRS, IPAG, 38000 Grenoble, France
[12]Institute for Research in Fundamental Sciences (IPM), School of Astronomy, Tehran, Iran
[13]Centro de Astrobiología (CSIC-INTA), Torrejón de Ardoz, 28850 Madrid, Spain
[14]Aix Marseille Univ, CNRS/IN2P3, CPPM, Marseille, France
[15]National Observatory of Athens, Institute for Astronomy, Astrophysics, Space Applications and Remote Sensing, Ioannou Metaxa and Vasileos Pavlou GR-15236, Athens, Greece
[16]Department of Astrophysics, Astronomy & Mechanics, Faculty of Physics, Univ. of Athens, Panepistimiopolis, GR-15784 Zografos, Athens, Greece
[17]High Energy Physics Division, Argonne National Laboratory, 9700 South Cass Av., Lemont, IL 60439, USA
[18]LERMA, Observatoire de Paris, PSL Research University, CNRS, Sorbonne Univ., UPMC, 75014 Paris, France
[19]Institute of Space Sciences (ICE), CSIC, Campus UAB, Carrer de Can Magrans s/n, E-08193, Barcelona, Spain
[20]ICREA, Pg. Lluís Companys 23, Barcelona, Spain
[21]IRAP, CNRS, Univ. de Toulouse, CNES, UT3-UPS, (Toulouse), France
[22]Dipartimento di Fisica, Univ. di Roma 'Tor Vergata', Via della Ricerca Scientifica 1, Roma, Italy
[23]School of Physics and Astronomy, University of Leeds, Leeds LS2 9JT, UK
[24]Institut d'Astrophysique de Paris, Sorbonne Université, CNRS (UMR7095), Paris, France
[25]Univ. de Lyon, UCB Lyon 1, CNRS/IN2P3, IP2I, 69622 Villeurbanne, France

© The Authors, published by EDP Sciences. This is an open access article distributed under the terms of the Creative Commons Attribution License 4.0 (https://creativecommons.org/licenses/by/4.0/).

Abstract. The N2CLS survey observed the GOODS-N and COSMOS fields at 260 GHz and 150 GHz with the NIKA2 camera, reaching the confusion limit in GOODS-N at 1.2 mm and approaching it at 2.0 mm. In this short proceedings, we present the results of the survey, including the source number counts, multi-wavelength SED fitting, the dust mass function, the evolution of the dust mass density, and the physical characterization of the detected galaxy population.

1 Introduction

Blind far-infrared (FIR) to millimeter (mm) surveys have dramatically improved our understanding of dusty star forming galaxies (DSFGs). The majority of the star formation at high redshift occurs in DSFGs, with the peak of galaxy growth, traced by the cosmic star formation rate density (SFRD), occurring at redshifts $1 < z < 3$ [1]. Dust absorbs the ultraviolet emission of young OB-type stars and re-emits it at long wavelengths in the mid-infrared (MIR) and FIR spectral domains, up to the mm regime. Remarkably, the fraction of SFRD powered by luminous IR galaxies at $z > 4$ is as large as 60% [2]. Thus, studying the dust mass budget of high redshift DSFGs is key to have a comprehensive view of galaxy evolution.

The dust mass in a galaxy is dominated by large dust grains [3], that emit predominantly in the sub-mm and mm spectral ranges. Thanks to the negative k-correction of the Rayleigh-Jeans tail of dust emission, mm fluxes are not affected by cosmological dimming and distant luminous DSFGs are therefore favorably detected in mm blank field surveys [4].

The New IRAM KID Arrays 2 (NIKA2; [5, 6]) is a dual-band millimeter continuum camera operating at 1.2 and 2.0 mm, installed at the IRAM 30m telescope in Spain. It consists of three arrays of kinetic inductance detectors, two at 1.2 mm (1140 detectors each) and one at 2.0 mm (616 detectors), with a field of view of ~ 6.5 arcmin in diameter.

As part of the guaranteed time program, the NIKA2 Cosmological Legacy Survey (N2CLS; PIs G. Lagache, A. Beelen, N. Ponthieu) observed the GOODS-N and COSMOS fields [7, 8] to obtain a systematic census of DSFGs at 1.2 and 2.0 mm. A total of 86 and 195 hours of telescope time were dedicated to GOODS-N ($\sim 160\,\mathrm{arcmin}^2$) and COSMOS ($\sim 1030\,\mathrm{arcmin}^2$), respectively. We present here the first results of the survey.

2 N2CLS data

The reduction of the NIKA2 data was carried out with the IRAM PIIC software [9, 10] and the custom IDL pipeline [11], following the iterative procedure for deep fields [4]. The NIKA2 maps of GOODS-N reach average noise levels of 0.17 mJy/beam, and 0.047 mJy/beam at 1.2 and 2.0 mm, respectively. The COSMOS maps reach an average r.m.s. of 0.32 mJy/beam and 0.10 mJy/beam, in the two bands [4, 12]. At the GOODS-N depth, NIKA2 is within a factor of 2 from the confusion limit at 1.2 mm and 2.0 mm [11].

Source extraction was performed by identifying the sources on match-filtered maps and measuring fluxes via PSF-fitting. A total of 120 and 67 sources in GOODS-N and 301 and 124 sources in COSMOS maps were detected at 1.2 and 2.0 mm, respectively. Artificial sources were added to the NIKA2 timelines with the aim to study the completeness and reliability of the source catalogs, as well as correct flux boosting/filtering. In GOODS-N, the catalogs reach a purity of 80% at S/N$\sim$3.0, and $>$ 95% at S/N$>$4.2. In COSMOS, they reach 80% purity at S/N$\sim$3.9, and $>$ 95% at S/N$>$4.5 for 1.2 mm and S/N$>$4.6 for 2.0 mm [4, 12].

Figure 1 presents the 1.2 and 2.0 mm N2CLS number counts, compared to literature data. Source counts are transformed into galaxy counts using the SIDES [13] simulation to evaluate the effect of blending onto the NIKA2 data. N2CLS defined the number counts with unprecedented precision, thanks to the systematic coverage of the two large areas [4].

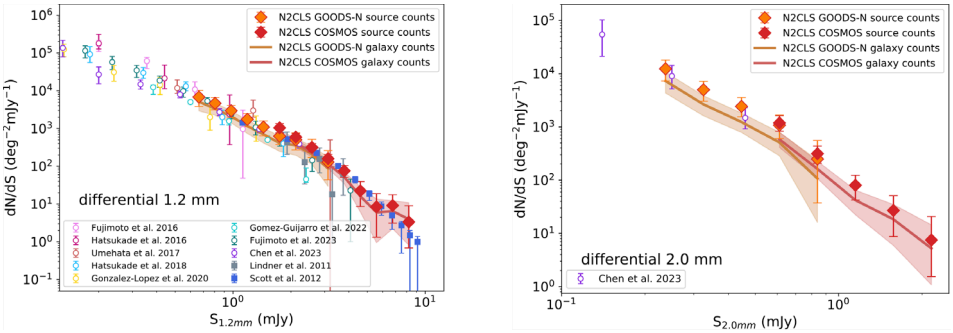

Figure 1. Differential N2CLS number counts at 1.2 mm (*left*) and 2.0 mm (*right*), compared to the literature [4, and references therein].

3 Multi-wavelength analysis of GOODS-N

The GOODS-N field benefits from a very rich multi-wavelength database spanning from X-rays to radio frequencies and including observations with all major space telescopes and ground-based facilities. We cut the NIKA2 catalog at the 95% purity level and matched it to the available multi-wavelength data. We started from high-resolution sub-millimeter and radio observations of the Sub-millimeter Array (SMA) and Very Large Array (VLA), down to the near-infrared (NIR) and optical, through FIR and MIR. In case of missing high-resolution long-wavelength data or redshift estimates, we performed further millimeter interferometric observations with the IRAM NOrthern Extended Millimeter Array (NOEMA).

The result of this heroic effort is a multi-wavelength catalog including up to 34 broad-band photometric measurements, spanning over the wavelength range from 3600 Å to 21 cm. It includes a total of 68 individual galaxies with redshifts between $z = 0.6$ and $z = 7.2$.

We exploited this exceptional data set to fit the spectral energy distributions (SEDs) of these galaxies with state of the art models [14]: modified black body (MBB) and Draine & Li [15, DL07] models in the FIR-mm spectral range [16]; MAGPHYS, SED3FIT and CIGALE models from the UV to the radio [17–19].

4 Dust mass function and density evolution

The main product of SED fitting is the dust mass, $M_{\rm dust}$, of the N2CLS GOODS-N galaxies. Applying the $1/V_a$ method [20], the comoving number density of the sources in intervals of $M_{\rm dust}$, also known as dust mass function (DMF), was computed. The mass completeness of the sample was evaluated by studying the mm flux distribution in intervals of $M_{\rm dust}$ and assuming that the same distribution holds above and below the adopted flux density cut [14].

We describe the DMF with a Schechter function in logarithmic form [21]. The Schechter parameters that best describe the observed DMF were derived by applying the STY (Sandage, Tammann, & Yahil) method [22]. By integrating the Schechter function in three redshifts bins ($1.6 < z \leq 2.4$, $2.4 < z \leq 4.2$, and $4.2 < z \leq 7.2$), we studied the evolution of the dust cosmic density, $\rho_{\rm dust}$, of DSFGs.

Figure 2 presents the DMF (left panel) and the dust cosmic density (right panel) evolution [14], including literature data and theoretical models from the local Universe to the cosmic dawn. When comparing to existing data, it is paramount to scale them all to the same dust mass absorption coefficient κ_ν(dust), because $M_{\rm dust}$ depends inversely on it. The adopted reference is $\kappa_{850\mu m} = 0.047$ m^2 kg^{-1} [23].

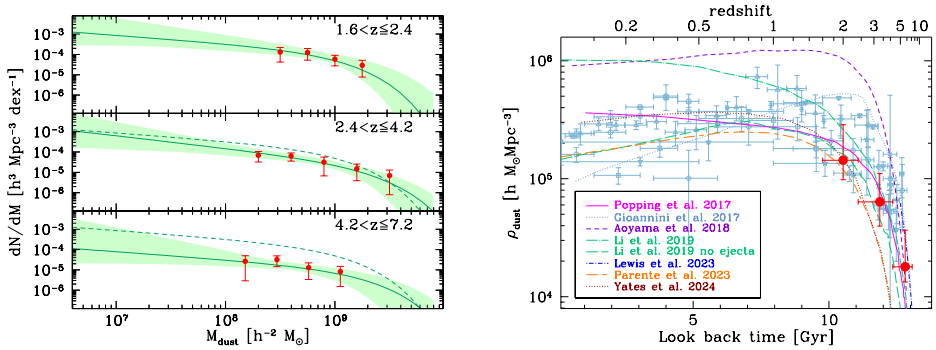

Figure 2. Evolution of the dust content of the DSFGs [14]. *Left panel*: DMF of the N2CLS GOODS-N galaxies (red symbols). The green solid lines and shaded areas are the result of the STY Schechter parametric analysis. The dashed green lines represent the $1.6 < z \leq 2.4$ result, repeated in the other two redshift bins for comparison. *Right panel*: evolution of the dust mass density as a function of look-back time, with N2CLS data (red symbols) compared to literature data and theoretical models (references in [14]). All data have been rescaled to our chosen cosmology and κ_ν(dust) [23]. The most successful models are those by [24] and [26] when excluding the dust expelled from the galaxies.

Combined to past literature results, our data reveal a two-fold evolution of the DMF of millimeter galaxies: *(a)* the characteristic density Φ^* rapidly doubles from $z \sim 7$ to $z \sim 2.5$, increases by a further factor of five at later epochs and ceases to evolve at $z \sim 0.5-1.0$; *(b)* the characteristic dust mass, M^*, keeps constant from $z \sim 7$ to $z \sim 4$ and then decreases smoothly by more than an order of magnitude down to the local Universe.

The comparison with simulations of dust and galaxy evolution favors semi-analytical and chemical evolution models that take into account dust growth and destruction [24, 25]. Hydrodynamical simulations are also successful when excluding the fraction of dust expelled into the inter-galactic medium from the dust budget of the galaxies [26].

5 The nature of the NIKA2 GOODS-N DSFGs

The panchromatic UV-to-radio SED fitting produces also an estimate of the stellar mass, $M_\star$, and of the star formation rate, SFR, of the N2CLS galaxies. Adopting the scaling relation by [27], that links $M_\star$, redshift and distance from the main sequence (MS) of star forming galaxies to their molecular gas depletion timescale ($\tau_{\rm dep}$), we compute $\tau_{\rm dep}$ of the N2CLS galaxies. Figure 3 compares the result to a collection of data from the literature [14, 27, and references therein]. The N2CLS GOODS-N galaxies occupy mainly the locus of starbursts, with depletion timescales of the order of 0.1 to 1.0 Gyr.

Noteworthy, a remarkable overdensity of ten bright dusty star-forming galaxies at $z \sim 5.2$ exists in Fig. 3. [28] report that six of them are securely associated with the exceptional overdensity reported by [29] in GOODS-N. Moreover, five of these sources benefit from a spectroscopic determination of their redshift, including the famous first sub-mm galaxy discovered by SCUBA, HFD850.1 [30, 31].

These galaxies exhibit exceptional SFR ranging from 200 to 2000 $M_\odot$ yr^{-1} and large stellar masses ($10^{10} - 10^{12}$ $M_\odot$), placing most of them significantly above the $z \sim 5.2$ MS of star forming galaxies [27]. Their large dust masses, short gas depletion timescales, and high stellar baryon conversion efficiencies ($\epsilon_\star > 20\%$) indicate an early and rapid buildup of both

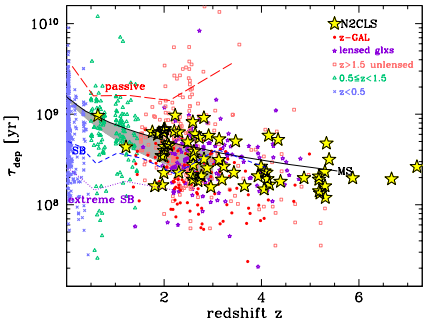

Figure 3. Depletion timescale of the N2CLS galaxies in GOODS-N, obtained applying the [27] scaling relation [14]. The grey shaded area is the trend found by [33]. The different lines represent the trends found by [27] for: main sequence galaxies (black solid line); starburst galaxies (blue dashed line); extreme starbursts (purple dotted line); below-MS galaxies (red long-dashed line). The list of references of all literature data is found in [14].

stellar and dust mass, comparable to what was found by [32] in $z > 5$ ultra-massive galaxies. These DSFGs could evolve into quiescent galaxies by $z \sim 4.5$, assuming no new gas inflow.

6 Summary

The N2CLS survey observed the GOODS-N and COSMOS fields at 1.2 and 2.0 mm with NIKA2, close to the confusion limit in GOODS-N [11]. The number counts thus obtained are the most precise so far at these wavelengths, thanks to the large and contiguous area of the covered fields [4, 12]. *Data and catalogs are publicly available at the survey web page*[1].

Matching the NIKA2 catalogs to the rich multi-wavelength data sets in GOODS-N, we built SEDs ranging from the UV to radio frequencies and we fitted them with state of the art models to derive the physical properties of these galaxies. Combined with previous results found in the literature, this allowed us to build the DMF and study the evolution of the dust cosmic density of DSFGs from $z \sim 7$ to the local Universe [14].

The evolutionary trends observed for the DMF and $\rho_{\rm dust}$ indicate a scenario in which DSFGs at "cosmic noon" are more numerous than at earlier epochs and contain more dust than their low-z cousins. This two-fold evolution can be explained with dust being rapidly produced in the distant Universe, heating up and emitting at FIR-millimeter wavelengths, thus peaking at $z = 2 - 3$, and finally being slowly and gradually consumed by star formation or expelled by galactic winds in more recent epochs, when dust production by AGB stars and supernovae does not balance the "losses" anymore [14].

Ten of the DSFGs detected by NIKA2 in GOODS-N are concentrated around $z \sim 5.2$ and belong to the HDF850.1 known overdensity studied by [29]. Their short $\tau_{\rm dep}$ and high stellar baryon conversion efficiencies [28] imply that NIKA2 is witnessing the early formation of massive quiescent galaxies in a dense environment.

In order to reduce the scatter now present in the $\rho_{\rm dust}$ evolution data, future deep studies will need to cover larger volumes and self-consistently encompass both low redshift regimes and rare very distant dusty galaxies.

Acknowledgements

We would like to thank the IRAM staff for their support during the observation campaigns. The NIKA2 dilution cryostat has been designed and built at the Institut Néel. In particular, we acknowledge the crucial contribution of the Cryogenics Group, and in particular Gregory Garde, Henri Rodenas, Jean-Paul Leggeri, Philippe Camus. This work has been partially funded by the Foundation Nanoscience

[1] N2CLS data and catalogs: https://data.lam.fr/n2cls.

Grenoble and the LabEx FOCUS ANR-11-LABX-0013. This work is supported by the French National Research Agency under the contracts "MKIDS", "NIKA" and ANR-15-CE31-0017 and in the framework of the "Investissements d'avenir" program (ANR-15-IDEX-02). This work has been supported by the GIS KIDs. This work has benefited from the support of the European Research Council Advanced Grant ORISTARS under the European Union's Seventh Framework Programme (Grant agreement No. 291294). R. A. acknowledges support from the Programme National Cosmology et Galaxies (PNCG) of CNRS/INSU with INP and IN2P3, co-funded by CEA and CNES. R. A. was supported by the French government through the France 2030 investment plan managed by the National Research Agency (ANR), as part of the Initiative of Excellence of Université Côte d'Azur under reference number ANR-15-IDEX-01. A. Maury acknowledges support the funding from the European Research Council (ERC) under the European Union's Horizon 2020 research and innovation programme (Grant agreement No. 101098309 - PEBBLES)

References

[1] P. Madau, M. Dickinson, ARA&A **52**, 415 (2014)
[2] Y. Khusanova, M. Bethermin, O. Le Fèvre et al., A&A **649**, A152 (2021)
[3] F. Galliano, Habilitation Thesis (2022), arXiv:2202.01868
[4] L. Bing, M. Béthermin, G. Lagache et al., A&A **677**, A66 (2023)
[5] L. Perotto, N. Ponthieu, J.F. Macías-Pérez et al., A&A **637**, A71 (2020)
[6] R. Adam, A. Adane, P.A.R. Ade et al., A&A **609**, A115 (2018)
[7] M. Dickinson, GOODS Legacy Team, *The Great Observatories Origins Deep Survey (GOODS)*, in *American Astronomical Society Meeting Abstracts, Vol. 198* (2001)
[8] N. Scoville, H. Aussel, M. Brusa et al., ApJS **172**, 1 (2007)
[9] R. Zylka, *MOPSIC: Extended Version of MOPSI, Astrophysics Source Code Library, record ascl:1303.011* (2013), https://ui.adsabs.harvard.edu/abs/2013ascl.soft03011Z
[10] S. Berta, R. Zylka, *Welcome to the PIIC*, https://www.iram.fr/~gildas/dist/piic.pdf
[11] N. Ponthieu, F.X. Désert, A. Beelen et al., A&A (2025), subm.
[12] M. Béthermin, G. Lagache, C. Carvajal-Bohorquez et al., arXiv e-prints arXiv:2506.22046 (2025)
[13] M. Béthermin, H.Y. Wu, G. Lagache et al., A&A **607**, A89 (2017)
[14] S. Berta, G. Lagache, A. Beelen et al., A&A **696**, A193 (2025)
[15] B.T. Draine, A. Li, ApJ **657**, 810 (2007)
[16] S. Berta, D. Lutz, R. Genzel et al., A&A **587**, A73 (2016)
[17] E. da Cunha, S. Charlot, D. Elbaz, MNRAS **388**, 1595 (2008)
[18] S. Berta, D. Lutz, P. Santini et al., A&A **551**, A100 (2013)
[19] D. Burgarella, V. Buat, J. Iglesias-Páramo, MNRAS **360**, 1413 (2005)
[20] M. Schmidt, ApJ **151**, 393 (1968)
[21] P. Schechter, ApJ **203**, 297 (1976)
[22] A. Sandage, G.A. Tammann, A. Yahil, ApJ **232**, 352 (1979)
[23] B.T. Draine, G. Aniano, O. Krause et al., ApJ **780**, 172 (2014)
[24] G. Popping, R.S. Somerville, M. Galametz, MNRAS **471**, 3152 (2017)
[25] L. Gioannini, F. Matteucci, F. Calura, MNRAS **471**, 4615 (2017)
[26] Q. Li, D. Narayanan, R. Davé, MNRAS **490**, 1425 (2019)
[27] L.J. Tacconi, R. Genzel, A. Sternberg, ARA&A **58**, 157 (2020)
[28] G. Lagache, M. Xiao, A. Beelen et al., arXiv e-prints arXiv:2506.15322 (2025)
[29] F. Sun, J.M. Helton, E. Egami et al., ApJ **961**, 69 (2024)
[30] D.H. Hughes, S. Serjeant, J. Dunlop et al., Nature **394**, 241 (1998)
[31] F. Walter, R. Decarli, C. Carilli et al., Nature **486**, 233 (2012)
[32] M. Xiao, P.A. Oesch, D. Elbaz et al., Nature **635**, 311 (2024)
[33] A. Saintonge, D. Lutz, R. Genzel et al., ApJ **778**, 2 (2013)